

Plasma Excitation in a DC Linear Magnetic Field by a Duoplasmatron Plasma Cathode

Jhoelle Roche M. GUHIT, Arnold Rey B. GINES, Kenta DOI and Motoi WADA

Graduate School of Science and Engineering, Doshisha University, Kyotanabe, Kyoto 610-0394, Japan

(Received 17 May 2020 / Accepted 25 May 2020)

A 280 G linear magnetic field sustained a 2.5 mm diameter stable hydrogen plasma column produced by a duoplasmatron plasma cathode. A high-intensity magnetic field created by a pair of permanent magnets and the field compression structure realized the passage of a dense plasma flow through a 2 mm diameter hole. Both ions and electrons can be extracted from the downstream plasma where a linear magnetic field can be induced to guide the plasma for striking a tungsten target. Luminous intensity distribution around a tungsten target located at another end of the magnetic field confronting to the plasma cathode was examined. A substantial reduction in the $H\alpha$ line spectral broadening was observed that enabled a precise spectroscopic study of the hydrogen particle reflection at the solid target surface.

© 2020 The Japan Society of Plasma Science and Nuclear Fusion Research

Keywords: particle reflection, tungsten, duoplasmatron ion source, plasma cathode

DOI: 10.1585/pfr.15.1401048

1. Introduction

Fundamental processes in plasma material interactions are often investigated using a linear device with an electron emission cathode for quasi-steady-state operations [1, 2]. A small device driven by a high-temperature tungsten cathode was developed to study $H\alpha$ line spectrum profiles that are Doppler-broadened due to particle reflection at a metal surface in a hydrogen plasma [3]. The line of sight for the measurement was set outside of the plasma to reduce noise due to photon emissions from the plasma. The measured spectra showed clear broadening corresponding to the velocity distributions of reflected particles when their incident energies were higher than 200 eV.

The observed spectrum showed a substantial broadening that could not be explained by the particle reflection at the target; the spectrum showed broadening at the skirt part even at low (less than 150 eV) hydrogen ion bombardment energy. The large plasma radius and the exposed target area may cause the velocity and the angular distributions of both incident and reflected hydrogen particle to vary and thus can enlarge the broadening of the $H\alpha$ line spectrum. Meanwhile, a smaller diameter plasma is preferred because the line of sight for the spectroscopic measurement should be set as close to the particle emission point as possible. A duoplasmatron source can produce intense plasma that can pass through an aperture less than 0.13 mm diameter [4]. This small size plasma ball can produce both ions and electrons depending upon the extraction voltage. In this report, we couple a small duoplasmatron source to a linear magnetic field to sustain small diameter plasma.

2. Methods

A duoplasmatron ion source was developed to replace a standard high-temperature filament driven plasma cathode source from the previous setup [3]. Figure 1 shows the experimental arrangement with the duoplasmatron plasma source that looks nearly identical to the original setup used for plasma bombardment onto a fuzzy tungsten surface [5]. This is because the main part of the plasma source for both setups is covered by the first electromagnet. In fact, even though the structure of the current duoplasmatron is more complicated than the previous plasma cathode, the length was much shorter; the length of the duoplasmatron plasma cathode from the filament to the extraction electrode is 86 mm while that of the previous plasma cathode

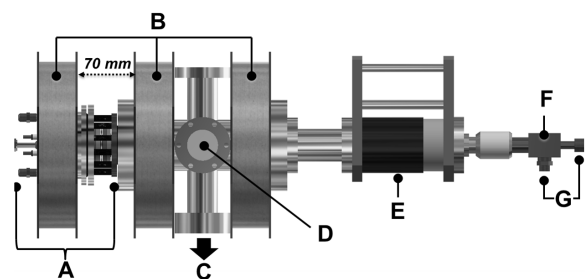


Fig. 1 Duoplasmatron plasma source experimental setup. **A** The duoplasmatron plasma cathode source for the discharge device. **B** Three electromagnetic coils to provide a linear magnetic field. **C** Port for vacuum pumping. **D** ICF 70 viewing port for spectroscopic and luminosity intensity measurements. **E** Manipulator for target holder to adjust the target distance from the center chamber. **F** Target electrical bias connection. **G** In and out water-cooling ports for backside cooling of the target.

from the filament to the flange of the downstream chamber is 144 mm [3]. Two more electromagnetic coils produce a linear magnetic field to guide the ionizing electrons.

Figure 2 shows the structure of the duoplasmatron plasma source. The operation of the source is illustrated using the alphabet A through F indicated in Fig. 2. A pair of current feed-through sustains a 0.40 mm diameters tungsten filament, **A**, for thermionic emission of ionizing electrons. The discharge is initiated between the filament and the conical water-cooled stainless-steel (SUS304) electrode, **B**. The ignition anode is a cone-shaped conduit with dimensions of ϕ 83 mm \times ϕ 13 mm \times 33 mm. Once the discharge is initiated, the plasma electrons penetrated a region formed by a mild steel made intermediate electrode, **C**. The intermediate electrode is made of iron and has the volume of conical shape with the dimensions of ϕ 6 mm \times ϕ 3 mm \times 10.5 mm. The electrical register connected to the cone shaped conduit biases the conduit at a floating potential drawing little discharge current from the primary discharge power supply (PPS). Thus, the conical electrode ignites the plasma, but the main part of the discharge current runs between the tungsten filament and the intermediate electrode. The current from the tungsten filament cathode passes through a 3 mm diameter hole opened at the center of the intermediate electrode and touches down the anode plate, **D**, as the switch connecting the intermediate electrode to the anode is opened.

The anode is an SUS304 circular plate with a 2 mm diameter tapered aperture. A pair of Nd-Fe ring magnets creates an intense magnetic field (estimated to be more than

4.5 kG [6]) in the region between the intermediate electrode and extraction electrode, **F**, to compress magnetically the plasma reaching the anode. This process completes the formation of a duoplasmatron plasma, and the dense plasma is ready to be extracted from the mild steel made extraction electrode with the inner volume ϕ 6 mm \times ϕ 3 mm \times 6.5 mm facing the anode. The PPS delivers a discharge current, I_{D1} , of typically 1 A and discharge voltage, V_{D1} , of 110 V in a usual operation. Filament power is maintained at 184 - 186 W to sustain the discharge current of 1 A.

Both electrons and positive ions can be accelerated from the plasma source by simply switching the polarity of the secondary discharge power supply, SPS. The spacing between the plasma source anode and the extraction electrode is 1 mm while the diameter of the extraction hole is 3 mm. The 2 mm thickness extraction electrode is tapered by a 45-degree angle at the side facing the extraction electrode. This part of the anode works as the expansion cup to control the local plasma density low enough to extract charged particles [7]. A strong inhomogeneity in the axial magnetic field intensity is created in the extraction region, because the extractor is made of magnetic material (mild steel). A double layer is known to be produced in this magnetic field configuration [8], and the plasma self-bias effect was often observed depending upon the polarity of the secondary discharge power supply; the plasma source acquires the potential as the power supply is protected against the reverse electrical current flow.

The extracted charged particle beam forms a plasma in the downstream area where a magnetic field is induced by electromagnets. A stable plasma is produced as electrons are extracted from the plasma source with input coil current, I_{coil} , from 7.5 - 15 A corresponding to the magnetic field intensity from 140 to 280 G. The plasma guided by the magnetic field extends up to the target normally located at 12 cm downstream of the extraction electrode, which is referred to as the standard position. The surface of the target can be adjusted by linear motion feedthrough along the direction of the magnetic field, while the target surface is observed from the tangential direction perpendicular to the field through two viewing ports with the center axis aligned to the surface center of the target located at the standard position.

In Fig. 2, the electrical wiring connection is shown when electrons are extracted from the duoplasmatron source. The SPS extracts electrons from the plasma cathode forming a sharp downstream plasma. A sheet metal target is attached to a water-cooled target support to be irradiated the surface by the plasma from the direction 45-degrees to the surface normal. The target can be electrically biased with respect to the plasma using a Target Bias Power Supply (TBPS).

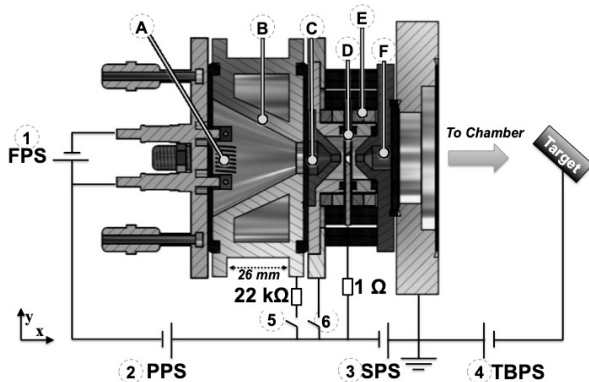


Fig. 2 Duoplasmatron plasma cathode source electrical schematic diagram. The horizontal and vertical orientation of the device is labeled as the x -axis and y -axis, respectively. **1** The filament power supply (FPS) for primary electron emission. **2** Primary discharge power supply (PPS) for primary discharge current production. **3** Secondary power supply (SPS) for secondary extraction. **4** Target bias power supply (TBPS). **5** primary switches. **6** Secondary switch. **A** Tungsten filament (a 7 turn coil with a 6 mm diameter of 0.4 mm diameter 155 mm length tungsten filament). **B** Ignition anode. **C** Intermediate electrode. **D** Anode. **E** Ring axial magnet (North-South x -axis orientation, ϕ 40 mm \times ϕ 30 mm \times 10 mm). **F** Extraction electrode.

3. Results

3.1 Discharge characteristics

The operation of the duoplasmatron as an ion source will be discussed later. The operation of the source as the plasma cathode is explained how to obtain the set original goal: production of sharp plasma. Once the duoplasmatron discharge is established after opening the secondary switch, 6 in Fig. 2, the hydrogen pressure was adjusted from 0.17 to 0.6 Pa to see the effect for the dependence of the primary discharge current upon the filament current.

The result in Fig. 3 shows the same primary discharge current was obtained gradually up to 0.17 Pa hydrogen pressure for the same filament heating power, while more filament heating power was necessary for operation at higher pressure. As a substantial increase in heating power was required for operation with hydrogen pressure higher than 0.2 Pa, the pressure was kept at this value to examine the performance of the cathode.

As we apply the secondary discharge voltage, V_{SPS} between the duoplasmatron anode and the extraction electrode, electrons are extracted to form an ionizing electron beam toward the downstream of the extractor. The current flowing the secondary discharge power supply, I_{D2} , was almost equal to the discharge current, I_{D1} , driving the duoplasmatron discharge. In Fig. 4, the discharge current ratios, I_{D2}/I_{D1} , and the floating potentials of the tungsten target are plotted as functions of V_{SPS} for two values of discharge current: $I_{D1} = 0.5$ A and $I_{D1} = 1.0$ A. As shown in the figure, the same magnitude of electrical current flows the secondary discharge power supply, even with no bias current. The ratio almost equates to 1 even for increasing V_{SPS} .

The magnetic field intensity that guides I_{D1} through the anode to make it as I_{D2} is far much greater than the linear magnetic field induced by electromagnets. The data shown in Fig. 4 was taken without inducing current to the electromagnets, but the identical characteristics were measured when the current was applied to the electromagnets. The produced plasma downstream of the duoplasmatron

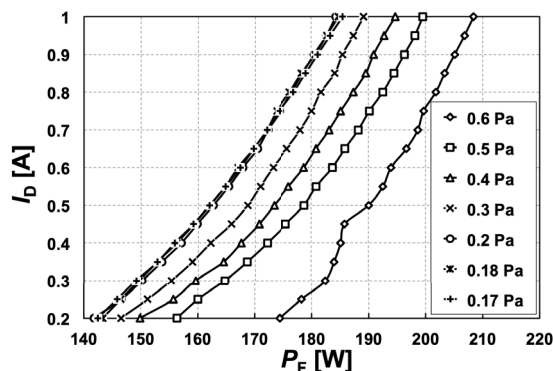


Fig. 3 Discharge Current (A) vs Filament power (W) for varying chamber pressure (hydrogen). [I_{D1} : 1 A, V_{D1} : 110 V, I_{coil} : 0 A, V_{SPS} : 0 V].

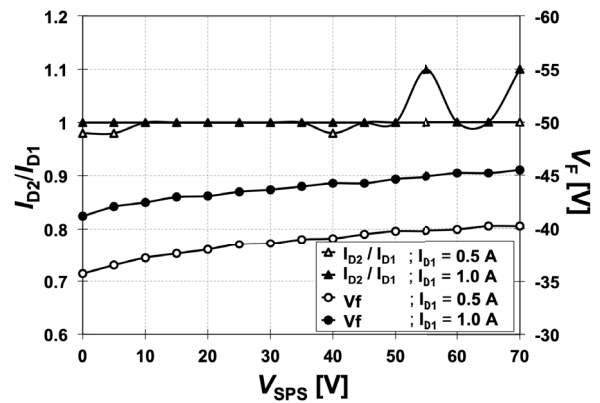


Fig. 4 I_{D2}/I_{D1} vs V_{SPS} and V_F (secondary axis) vs V_{SPS} : Discharge characteristics of duoplasmatron plasma cathode source. [I_{D1} : 1 A, V_{D1} : 110 V, I_{coil} : 0 A, V_{SPS} : 0 - 70 V negative bias].

anode is biased negatively using a secondary power supply (V_{SPS}) to transfer the electron to the chamber. The positive terminal of the V_{SPS} is grounded to the chamber. The current ratio I_{D2}/I_{D1} was measured to be slightly smaller than one when the primary discharge current was kept at 0.5 A, while it tended to be slightly larger than one at higher V_{SPS} with $I_{D1} = 1.0$ A. The accuracy in the measurement for taking data of Fig. 4 was one percent. The reason for the observed data scattering is attributable to the change in discharge condition when the V_{SPS} is varied.

The floating potential of the tungsten target became more negative with the increasing V_{SPS} and larger I_{D1} . Based upon the data of hydrogen ionization cross-section [9], the secondary discharge potential was set at 70 V in the following experiment to make the electron impact energy above the maximum for the cross-section to ionize hydrogen.

3.2 Luminosity intensity distribution

Figure 5 compares the difference in sizes of the plasma column produced by the previous plasma cathode (Fig. 5 A), and the present duoplasmatron plasma cathode (Fig. 5 B). The tungsten target was withdrawn out of the region observable through the viewing port. All pictures were taken in a batch process to make sure that all analyzed locations are the same. The image data are converted to 8-bit grayscale and pixel data were integrated to construct a luminous intensity distribution along the y-axis perpendicular to the magnetic field line of force. The diameter of the plasma glow column was more than 1 cm in the previous experimental system with the tungsten filament excited plasma cathode depending on magnetic field compression. Note that Fig. 5 is tilted by 90-degree to quantify the luminous intensity distribution for the measurement of the radius of the ionizing electron flowing channel. As indicated in the figure, a luminous intensity distribution is obtained by averaging the signal along the width indicated by the label 'a' extending in x, or the horizontal direction. The label 'b' is assigned to show the direction toward the

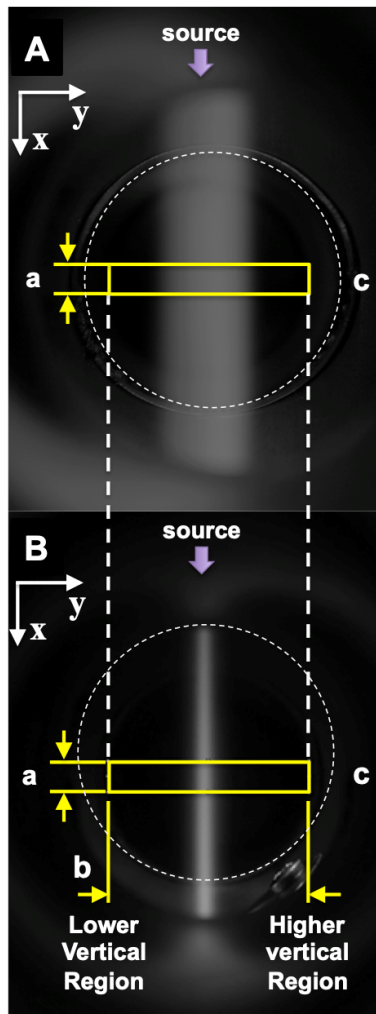


Fig. 5 Plasma glow for the **A**: previous plasma cathode [3] and **B**: Duoplasmatron plasma cathode [I_{D1} : 1 A, V_{D1} : 110 V, I_{coil} : 15 A, V_{SPS} : -10 V, and no target bias]. The plasma flow is from the arrow indicated (x -axis). **a**: Region for averaging of the plasma drift direction with grayscale unit scale. **b**: Lower region indicates the lower y -axis of the plasma region **c**: Reference of the 34 mm diameter (actually measured) circle opened on the inner wall of chamber connected to a stainless-steel tube holding the ICF-70 viewing port at the other end.

bottom, where the surface of the tungsten target is located away from the center of the viewing port. The vertical y coordinate has the origin at the plasma center and is more negative toward the label 'b'. The circle 'c' is drawn as a reference of the 34 mm diameter opening on the stainless-steel chamber welded to the tube to hold the ICF-70 size viewing port flange.

The pixel data converted to show the luminous intensity distribution along the y -axis are shown in Fig. 6. The diameter of the plasma glow column was more than 1.2 cm in the previous experimental system in which a tungsten-filament-driven plasma served as the discharge cathode. The spatial inhomogeneity as observed in the image of Fig. 5 A can be seen quantitatively as the shift of the brightest point from the axis by 2 mm in Fig. 6. Meanwhile, the

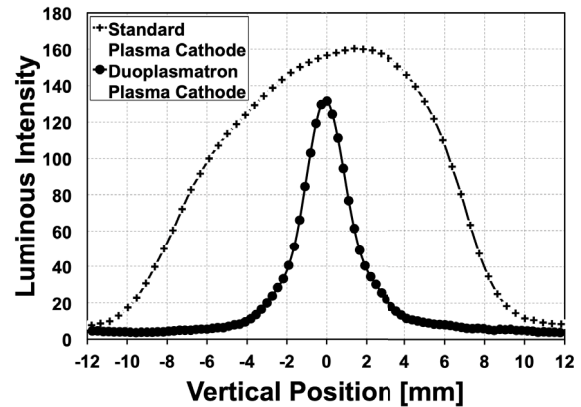


Fig. 6 Luminosity profile comparison between the duoplasmatron plasma cathode and the plasma cathode source (old setup). [I_{D1} : 1 A, V_{D1} : 110 V, I_{coil} : 15 A, V_{SPS} : -10 V].

present duoplasmatron source realizes far much sharper distribution without any shift from the center as shown in the figure. The intensity profile for the duoplasmatron plasma cathode shows a more symmetric distribution than the previous setup.

The luminous intensity distributions in the y -direction are plotted for different values of coil current to produce linear magnetic field keeping I_{D1} at 1.0 A. Voltage for SPS is -10 V. No distinct change in intensities for SPS input until -70 V. Hydrogen pressure is still sustained at 0.2 Pa. The magnetic field intensity, B , at the center of the tungsten target surface can be expressed by $B = 18.7 \times I_{coil}$ with I_{coil} being the current supplied to the electromagnets. Figure 7 A shows that the system can guide the plasma down to the target position with only less than a 2.5 mm displacement even without inducing the current to the electromagnets. This is because the pair of toroidal magnets forming the duoplasmatron magnetic field generates a straight magnetic field along the axis. The misalignment of the duoplasmatron field axis with respect to the linear magnetic field axis is estimated to be less than 1.4-degree.

As the electromagnetic coil current is increased, the profile starts to focus even with 2.5 A. A clear sharpening of the profile is observed starting at 10 A current to the electromagnets as indicated in Fig. 7 B. The maximum luminous intensity was observed at 7.5 A electromagnetic coil current. The reason for observing the maximum intensity at a reduced magnetic field intensity is unclear at this moment. A strong gradient of axial magnetic field intensity also exists at the region downstream of the extraction electrode like in the gap between the plasma source anode and the extractor. The formed double layer can enhance the local plasma loss at a higher field intensity, but this assumption should be tested by investigating the local plasma inside the constricted region. Increase in secondary extraction voltages did not affect the luminous intensity profile; the peak intensities and the width of the profiles were similar. Above more than 10 A coil current, a sharp plasma-glow column of less than 2.5 - 3.0 mm radius was realized.

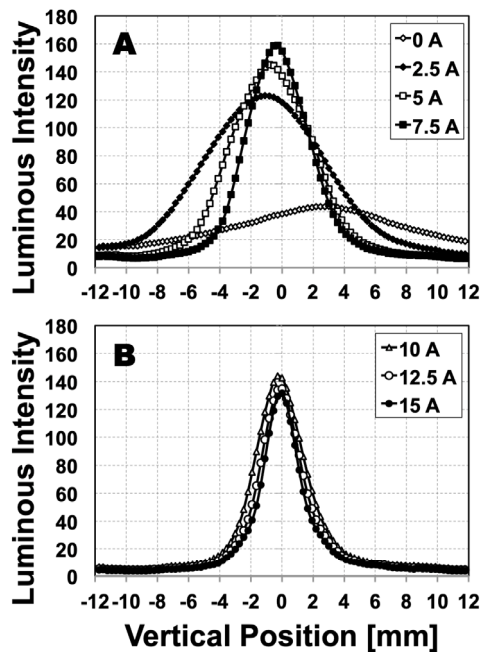


Fig. 7 Luminosity profile at varied secondary discharge voltages at increasing electromagnetic coil current. **A** 0 - 7.5 A electromagnet current input and. **B** 10 - 15 A electromagnet current input. [I_{D1} : 1 A, V_{D1} : 110 V, and V_{SPS} : -10 V].

3.3 $H\alpha$ wavelength spectrum

The tungsten target was placed at the spectroscopic measurement position and biased at -100 V with respect to the plasma formed in the downstream chamber and the plasma was excited with $I_{D1} = 1.0$ A and $B = 280$ G with the secondary extraction voltage maintained at -10 V and hydrogen pressure at 0.2 Pa. A substantial reduction of the line broadening at the skirt part of the $H\alpha$ spectrum has been achieved as shown in Fig. 8 that compares the $H\alpha$ spectral shapes obtained with both plasma cathodes. The monochromator resolution calibrated by a 1 mm radius hydrogen gas discharge lamp was 23 pm while the spectrum was taken with the duoplasmatron cathode plasma still exhibits 35 pm full-width at the half maximum. This reduced spectrum width from 60 pm for the plasma excited by the previous system enabled the observation of the Doppler broadening at the skirt part of the measured $H\alpha$ spectrum as indicated in Fig. 8.

4. Discussion

The spectrum shown in Fig. 8 exhibits an asymmetric broadening with the blue wing shorter than the red wing. Assuming 75 pm as the end of the blue wing, the corresponding hydrogen atom energy is to be 12 eV. In the previous system, spectrum analysis at this low energy range was impossible due to a severe broadening of the tail part. The operation of the duoplasmatron cathode reduces the hydrogen gas pressure in the measurement region, which should reduce hydrogen ion charge exchange reaction leading to the formation of high-energy atoms

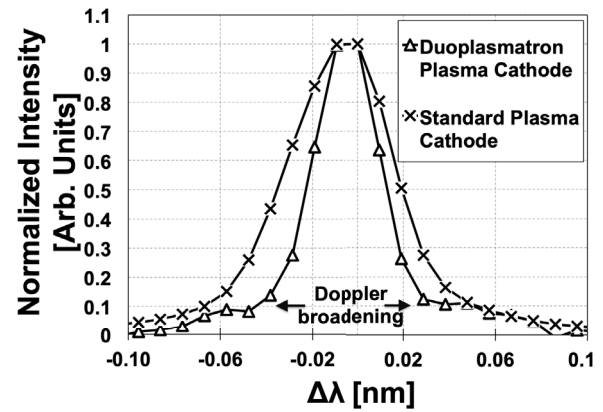


Fig. 8 Comparison of the particle reflection between the duoplasmatron plasma cathode device (new ion source device) and standard high-temperature DC cathode source (old ion source device) at -100 V target bias voltage. [I_{D1} : 1 A, V_{D1} : 110 V, and I_{coil} : 15 A].

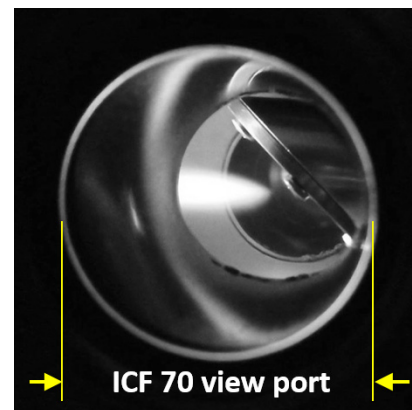


Fig. 9 Duoplasmatron plasma cathode device with plasma termination is observed at -600 V target bias voltage applied to the target. [I_{D1} : 1 A, V_{D1} : 110 V, I_{coil} : 7.5 A, V_{SPS} : -10 V].

to emit photons of Balmer- α wavelength. The contribution from the surface area on the target reflecting incoming ions is one to two orders of magnitude smaller than that from the plasma created by the duoplasmatron source. This smaller area of fast hydrogen atom emission can result in sharper velocity (energy and angular) distribution of atomic hydrogen along the observation axis of the spectrometer. A comparison between the observed spectrum and the velocity distribution obtained by computer simulation [10] is being made to see the effect of the target area.

Direct comparisons of the $H\alpha$ wavelength spectra with the previous plasma cathode discharge were attempted for higher bias voltages. The small diameter of the plasma column created by the duoplasmatron cathode showed a sensitive response to the negative bias applied to the tungsten target. Figure 9 shows the plasma glow when the target was negatively biased at -600 V. The figure clearly shows that the produced plasma does not reach the target, while the diameter appears far larger than the one shown in Fig. 5 for the case that the target is withdrawn. As the

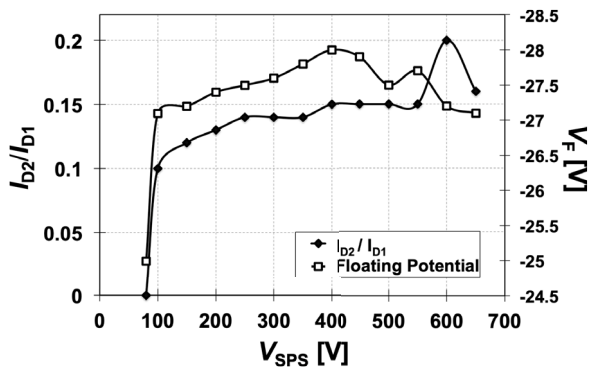


Fig. 10 I_{D2}/I_{D1} vs V_{SPS} and V_F (secondary axis) vs V_{SPS} : Discharge characteristics of duoplasmatron for positive extraction. [I_{D1} : 0.5 A, V_{D1} : 110 V, I_{coil} : 0 A, and V_{SPS} : 100 - 650 V].

target surface intersects the axis of the plasma guided by the linear magnetic field forming a 45-degree angle, the produced electric field across the sheath seemed to cause a plasma instability near the target. A precise study on the frequency and the density spatial distribution is still under way, but the plasma luminous intensity measurements like Fig. 9 clearly show the extinction of plasma glow near the target at a higher voltage target bias.

A duoplasmatron source was originally developed as a high current density positive ion source with the extractable ion current so high that the reduction of the local ion density was necessary to form an ion beam from the plasma passing through the extraction hole [11]. The present extraction spacing is far much smaller than the original designs and may not be appropriate for ion extraction. We tried to apply a positive bias to the source for testing if the ion current can be extracted from the plasma source.

Once the SPS electrically reconnected, with positive bias input voltage and negative bias grounded to the chamber, to extract positive ions was connected, there appeared an 80 V self-bias potential between the extractor and the duoplasmatron anode as shown in Fig. 10. By applying an extraction potential, the extraction current immediately saturated at 70 mA above 400 V for 0.5 A discharge current. Further increase in extraction voltage resulted in a breakdown at the extractor (only 1 mm gap between the anode and the extractor) and the operation above 400 V was unstable.

However, because of the observed characteristics of positive voltage self-bias, positive ions are expected to pass through the plasma expansion area downstream of the anode. They produced a dilute plasma downstream, and the tungsten target showed a negative floating potential indicating the ion beam reaching the target was smaller than

the thermal electron current from the ion beam produced plasma. Part of the reason for the inefficient positive ion transport down to the target is the large beam divergence of this type of ion source for the operation with a low extraction potential [12]. The extraction geometry has to be modified if the present source will serve as a positive ion source.

5. Conclusions

A compact duoplasmatron source was designed and used as the plasma cathode for exciting plasma in a linear magnetic field. A plasma column with a sharp boundary has been successfully produced, and the improvement in the accuracy of Doppler broadening measurement was realized. By collecting more information on broadening by observing pressure dependence and plasma size dependence, the reason for observing unexpected broadening at the skirt part of the $H\alpha$ line spectrum is expected to be clarified. The formed narrow ionizing electron channel is found sensitive to the local electric field near the target, and the preparation of a target with the surface intersecting the magnetic field perpendicularly can stabilize the plasma transport down to the target surface. The designed source also has the potential to serve as a hydrogen positive ion source that delivers ion current to the target. The direct reflection of ions from the source will be investigated spectroscopically after some necessary modifications for the ion extraction are made.

- [1] D.M. Goebel, G. Campbell and R.W. Conn, *J. Nucl. Mater.* **121(C)**, 277 (1984).
- [2] M.Y. Ye, S. Takamura and N. Ohno, *J. Nucl. Mater.* **241-243**, 1243 (1997).
- [3] K. Doi, H. Yamaoka, T. Kenmotsu and M. Wada, *IEEE Trans. Plasma Sci.* **46(3)**, 482 (2018).
- [4] C.D. Moak, H.E. Banta, J.N. Thurston, J.W. Johnson and R.F. King, *Rev. Sci. Instrum.* **30**, 694 (1959).
- [5] K. Doi, H.T. Lee, N. Tanaka, H. Yamaoka, Y. Ueda and M. Wada, *Fusion Eng. Des.* **136**, 100 (2018).
- [6] H. Takeuchi, Y. Yogo, T. Hattori, T. Tajima and T. Ishikawa, *ISIJ (Iron Steel Inst. Jpn.) International* **57**, 1883 (2017).
- [7] A. van Steenberg, *IEEE Trans. Nucl. Sci.* NS-12, 746 (1965).
- [8] R. Plamondon, J. Teichman and S. Torven, *J. Phys. D.* **21**, 286 (1988).
- [9] R.K. Janev, W.D. Langer, K. Evans, Jr. and D.E. Post, Jr. *Elementary Processes in Hydrogen-Helium Plasma* (Berlin, Heidelberg: Spiner-Verlag, 1987).
- [10] Y. Yamamura and W. Takeuchi, *Radiat. Eff.* **71**, 65 (1983).
- [11] L.E. Collins and R.J. Brooker, *Nucl. Instrum. Methods* **15**, 193 (1962).
- [12] T. Kuzumi and M. Wada, *Rev. Sci. Instrum.* **91**, 013505 (2020).